**Aldridge, John N.; Bacon, John C.; Dolphin, T.; Farcas, A.**

# Sediment dynamics of a nearshore sandbank: Results from TELEMAC-2D, TOMAWAC and SISYPHE modelling



# Sediment dynamics of a nearshore sandbank: Results from TELEMAC-2D, TOMAWAC and SISYPHE modelling.

J.N. Aldridge, J. C. Bacon, T. Dolphin, A. Farcas

Centre for Environmental Fisheries and Aquaculture Science, Pakefield Road, Lowestoft, Suffolk, NR33 OHT, john.aldridge@cefas.co.uk

***Abstract*— Results are presented from a model study of the sediment transport regime and morphological evolution of the Sizewell-Dunwich Bank, a headland associated sandbank on the east coast of the UK North Sea. Offshore sandbanks play an important role in reducing storm wave energy at the shoreline and the Sizewell-Dunwich Bank may be of particular importance for the stability of the neighbouring shoreline. To gain insight into possible bank evolution, calculations of tides, waves and sediment transport were made using the finite element TELEMAC model suite, with the aim of understanding bank formation and maintenance mechanisms. The general pattern of tidally averaged total transport flux (bedload plus suspended load) indicated a zone of convergence at the location of the present Sizewell Bank and evidence of a weaker one at the location of the Dunwich Bank to the north. In common with previous studies tidal asymmetry was found to be oppositely oriented on the inshore and offshore sides of the banks. This suggest a plausible mechanism for the bank formation and maintenance with material from the north or the south having the potential to accumulate at the bank location.**

## I. INTRODUCTION

Offshore sand banks can play an important role in influencing shoreline evolution and movement by attenuating the incident wave energy through the process of wave breaking and bed friction [1]–[6]. Assessing future shoreline stability in the vicinity of such sandbanks therefore requires taking account of possible changes to the sandbank position and morphology. Such a case study is presented here for the Sizewell–Dunwich bank located on the east coast of the UK North Sea. The working assumption is that the bank is a headland associated sandbank belonging to the nearby Thorpeness promontory. Explanations for the existence of headland associated sandbanks have focussed on the presence of tidal residual eddies [7]–[9], bedload convergences [10], and more generally with differing flood-ebb tidal asymmetry on the shoreward and seaward flanks of the bank [11]–[15]. Numerical modelling studies using idealised coastline geometry and tidal forcing typically show the formation of sandbanks on both sides of a headland [15], however in many cases sandbank formation is observed to be asymmetrical, with a larger bank forming preferentially on one side of the headland [11]. The Sizewell-Dunwich Bank is an extreme case with a substantial bank to the north of Thorpeness, but no bank observed to the south. The shape of the bank, pear shaped with the broader end pointed toward the headland and with steeper sides on the seaward flank at the broader end, is in remarkable accord with the description given in [13] for type 3A headland associated banner banks.

In this paper the mechanisms for formation and maintenance of the Sizewell-Dunwich Bank are investigated as a prelude to the eventual goal of predicting potential changes in bank morphology, evolution over decadal timescales. Results are presented for tidally averaged sediment transport fluxes both tidal and wave effects on the bedload and suspended load transport are considered and associated erosion and deposition patterns based on the recent bank configuration.

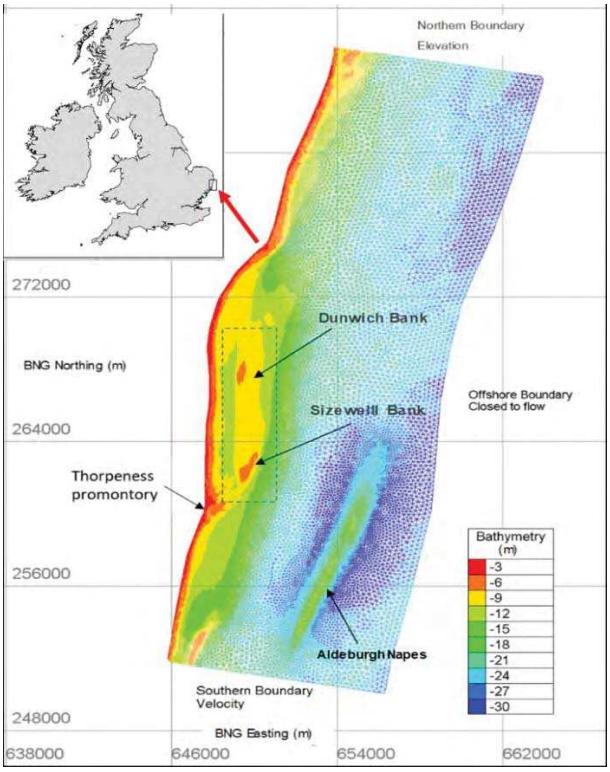


Figure 1: TELEMAC-2D model domain and mesh. The Sizewell-Dunwich Bank is indicated by the dashed box. Coordinate system is the British National Grid and elevations are in metres below ODN. Mesh resolution in the Sizewell-Dunwich Bank region is too high to discern individual elements but ranges from 30-50m elements on the bank increasing to 300m offshore.

## II. METHODS

Modelling in this study used the TELEMAC suite of models consisting of TELEMAC-2D, TOMAWAC and SISYPHE to simulate tides, waves and sediment transport respectively [17], [18],[23]. TELEMAC-2D and SISYPHE were run in fully coupled mode, so that bed elevation change calculated in the sediment transport model SISYPHE was feed back to the hydrodynamic model. TOMAWAC was run separately in non-coupled mode to provide surface wave amplitude and period. All models were run on a common finite element mesh and associated bathymetry covering the greater

Sizewell embayment (Figure 1). Depth data covering the region from the mouth of the Blyth River to Thorpeness, were obtained from high resolution (better than 10m horizontal resolution) surveys carried out between 2007 and 2009 [19]. This survey data was integrated with data from the UK Hydrographic Office for the offshore region. The combined dataset was corrected to Ordnance Datum Newlyn (ODN) as an approximation to the local Mean Sea Level (MSL). The highest mesh resolution was approximately 50m in the shallow inshore region adjoining Thorpeness and the Sizewell-Dunwich Bank, increasing to around 300m for the offshore regions. Bathymetric smoothing was applied using a Fourier transform method [20] to the raw depth values. This procedure removed mesh scale noise in the calculated erosion/deposition patterns evident when calculations were performed on an unsmoothed bathymetry.

A. *Hydrodynamics*

Tidal forcing consisted of surface elevation specified at the northern boundary and depth average velocities at the southern boundary. The eastern offshore boundary was configured to follow the tidal stream and treated as a solid boundary with no transverse flow. TELEMAC-2D was run with a 10 second timestep and with a constant bed roughness coefficient corresponding to a rippled sand bed [21]. Measurements covering a 30-day period in November/December of 2013 provided the southern and northern hydrodynamic boundary forcing. A set of synthetic tidal forcing data was also generated from the measured velocity and elevations by applying a tidal analysis based on a least squares fit to a set of underlying harmonic constituent [22] to extract the M2 (largest semi-diurnal), M4 (first non-linear harmonic) and Z0 (residual) constituents. These generally provide the leading order components important for tidal sediment transport, namely: correct overall magnitude of tidal bed stress provided by the M2 constituent and the first order contributions to tidal asymmetry provided by M4 and Z0 constituents [23], [24]. This forcing allowed exact M2 tidal averages to be extracted in the simulations aimed at understanding the underlying transport processes.

*Table 1: Wave forcing applied at the boundary of the TOMAWAC wave model. Hs values are those applied at the model boundary. Values measured at the bank are typically reduced by 20% compared to the boundary values due to attenuation by bed friction. Significant wave heights for given return periods were derived from a Weibull distribution fit to 30 years of hourly values at a location offshore of the Sizewell Dunwich bank taken from the UK Meteorological Office European Wave Model.*

| Case No | Wave direction (degrees from, North) | Hs (m) | Peak wave period (s) | Notes |
|---|---|---|---|---|
| **1** | 40 | 0.9 | 5.0 | Annual average NE[1] |
| **2** | 40 | 2.2 | 7.7 | 1 week return NE[1] |
| **4** | 153 | 0.94 | 4.0 | Annual average SE[2] |
| **5** | 153 | 2.2 | 6.0 | 1 week return SE[2] |

[1] From northeast sector. [2] From southeast sector.

B. *Waves*

Significant wave height (Hs), peak wave period (Tp) and were calculated using the TOMAWAC spectral wave model run on the same mesh as the hydrodynamic calculation with a time step of 10 seconds, 22 frequency bins and 36 wave directions. Water depths in the wave model were fixed with respect to Mean Sea Level (MSL) and did not include tidal variations. Observations from a wave rider situated offshore of the bank showed a strongly bi-model distribution of wave directions clustered around north easterly and south easterly directions. A set of four wave model runs were created (Table 1) by applying constant wave height and direction boundary forcing using two different wave heights for each of the two dominant wave directions. The TOMAWAC wave model was then run to steady state and the final results stored for later input to the coupled TELEMAC2D-SISYPHE model. Within the coupled model, wave height, period and water depth were combined, using linear water wave theory, to estimate the near-bed orbital velocity for sediment transport calculations.

C. *Sediment transport*

Information on sediments in the region was obtained from grab samples (grid resolution approximately 250m on the Dunwich Sizewell Bank and 500m off the bank), collected during March to April 2008. Surficial sediments in the region were found to be heterogenous, with areas of soft and compacted mud, fine to medium sands, gravels and regions of bare rock [25]. In contrast, the surface sediments of the bank were remarkably homogenous, consisting of well-sorted sands with median diameter 150 – 250 μm, straddling the boundary between fine and medium sands. No attempt was made to model the multi-particle size sediment dynamics of the entire region, instead the focus was on modelling the sediment associated with the Sizewell-Dunwich Bank. Model runs used a single size class of 250 μm. Sediment transport calculations used the SISYPHE model [26], [27]. This model allows the choice of a number of bedload and total load transport formulations, together with an option to calculate suspended load via an advection-diffusion transport equation. In this study bedload was calculated using the bedload component of the total load formulation of Soulsby and Van Rijn [21]:

$$Q_b = k_1 \overline{\mathbf{U}}[(|\overline{\mathbf{U}}|^2 + c_2 U_w^2)^{0.5} - U_{cr}]^{2.4} \quad (1)$$

where $\overline{\mathbf{U}}$ is the depth mean current vector, $U_w$ is the bed orbital velocity amplitude, $U_{cr}$ is a grain size dependent critical erosion velocity and $k_1$ is a grain size dependent coefficient, and $c_2 = 0.0036/C_D$ where $C_D$ is the 2D quadratic drag coefficient (set at a value appropriate for rippled sand [21]). This formulation was chosen as it includes both wave and current contributions. Note, the bedload vector is assumed to be aligned with the depth mean velocity. No slope correction was included in the sediment transport calculations. Tests with and without a slope correction made only a small difference to the overall prediction of bedload transport and associated erosion and deposition patterns. The

suspended load transport was calculated with the depth-integrated advection-diffusion equation

$$\frac{\partial C}{\partial t} + \beta\, \bar{\mathbf{U}}.\nabla C + D = -w_s(C_b - C_{ref})/h \qquad (2)$$

where $C$ is the depth mean suspended sediment concentration, $\bar{\mathbf{U}}$ is the depth mean current velocity, $h$ is the local water depth, $C_b$ is the predicted bed concentration derived from the depth mean concentration assuming a Rouse vertical profile. The factor $\beta < 1$ is a correction for the greater concentration of sediment near the bed and weights the advection velocity to be closer to a near-bed value. It is calculated at each time step assuming logarithmic and Rouse type profiles for velocity and sediment concentration respectively [31]. The reference concentration $C_{ref}$ is calculated from the bedload transport rate as described in [28] with

$$C_{ref} = Q_b/(b\ Z_{ref}\ u_*) \qquad (3)$$

Here $u_*$ is the bed friction velocity calculated from the skin friction component of the total stress derived from the sand grain roughness, the reference level $Z_{ref}$ is taken equal to the ripple roughness ($Z_{ref} = k_r$) and b=6.34 is an empirical constant. Ripple roughness ($k_r$) is calculated dynamically by SISYPHE based on the formulations of [29], [30]. Since $Q_b$ depends on both wave and current contributions (equation 1), the reference concentration and hence suspended load transport includes both wave and current forcing. Zero sediment flux for both bedload and suspended load was applied at the domain boundaries.

## III. RESULTS

For the results reported in this section, hydrodynamic boundary forcing was based on a tidal decomposition containing M2, M4 and Z0 (residual) constituents as described in Section 3.A. The coupled model was run for seven M2 tidal cycles. Time series plots indicated the model had reached a steady repeating state after two tidal cycles. The first two tidal cycles were discarded, individual bedload and suspended load vectors were summed and the net total load vectors were obtained by summing over five complete M2 tidal cycles. Associated net erosion and deposition was calculated over the same period. Off bank, the model was started with a uniform 10cm layer of 250 µm sand above a rigid non-erodible base. A thicker (5m) layer was placed on the bank. This case corresponds to an unlimited supply scenario since, other than right at the shore, the 10 cm layer was generally not eroded down to the rigid bed and was available as a sediment source (limited only by hydrodynamic forcing) to other locations. Thus, for the given hydrodynamic forcing, the sediment transport vectors presented here represent the potential maximum rates.

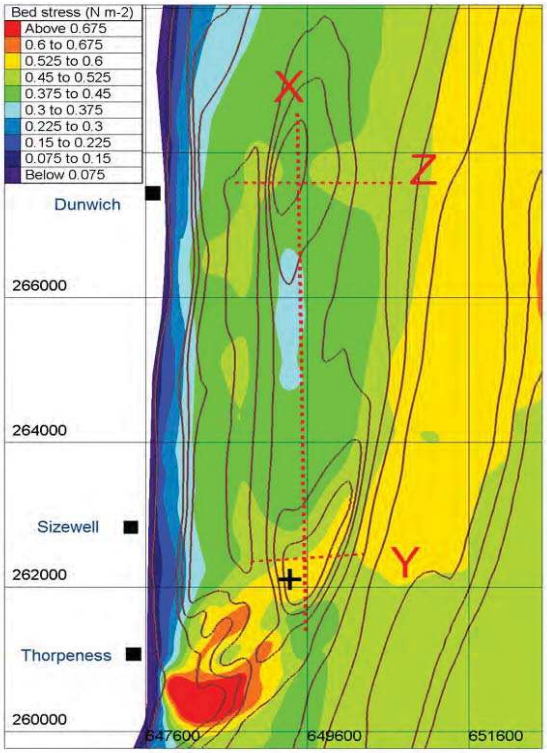


Figure 2: Tidally average bed stress values. Also indicated are the sections along which bed evolution is shown (Figure 12) and the position marked with cross (+) used to plot sediment flux and bed change over time (Figure 7).

### A. *Bed stress*

The tidal bed stress distribution in vicinity of the Sizewell-Dunwich Bank show a maxima just offshore of Thorpeness on the shallow platform and crag ridges, with a band of enhanced tidal stress extending along the southern and eastern faces of the bank (Figure 2). In the results shown later, this region shows relatively large changes in bed level. A minimum in bed stress occurs in the deeper 'swale' region between the Dunwich and Sizewell Banks and associated with relatively small morphology changes (see next section).

### B. *Erosion and deposition due to tidal forcing*

Model runs were carried out to assess the contributions of bedload, suspended load and wave-induced mobility to the modelled sediment flux and erosion/deposition patterns. Results are plotted as tidal averaged sediment flux vectors normalised (for display) to a uniform length to allow the net direction to be more easily discerned at smaller transport rates. Northward and southward pointing fluxes are coloured differently so that flood (south) and ebb (north) directed transport paths can be discerned.

The net bedload erosion and deposition are determined mathematically by the divergence of the net sediment transport flux vector. Although not exactly equivalent, broadly speaking deposition will occur when the average bedload magnitude decreases in the direction of net transport and erosion will occur when bedload magnitude increases in the direction of net transport.

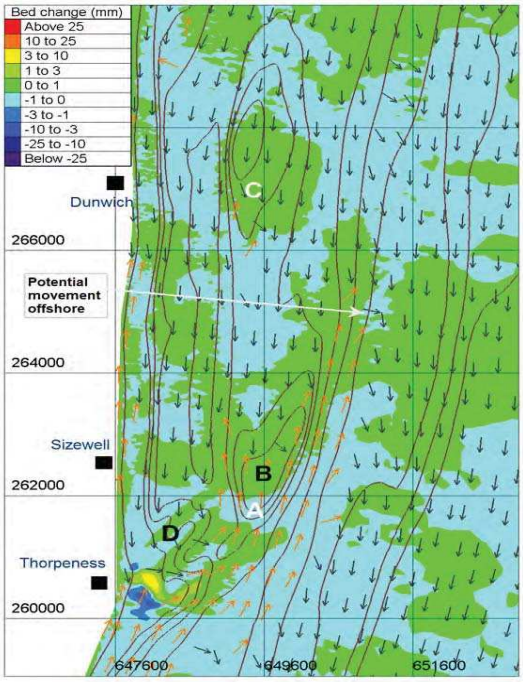


Figure 3: Bedload only with tidal forcing. Normalised tidal average transport vectors superimposed on erosion deposition patterns (mm) over five M2 tidal cycles for. Light coloured vectors represent net northerly (ebb) transport and dark vectors net southerly (flood) transport. Note, for clarity vector positions are sub-sampled and the plotted value is an average taken over the surrounding region. The actual mesh spacing is much denser.

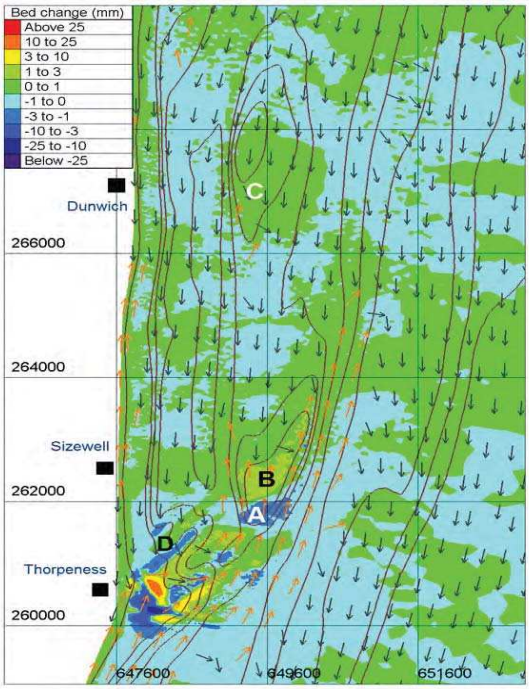


Figure 4: Bedload and Suspended load with tidal forcing. Normalised tidal average transport vectors superimposed on erosion deposition patterns (mm) over five M2 tidal cycles for. See Figure 3 for explanation of vectors.

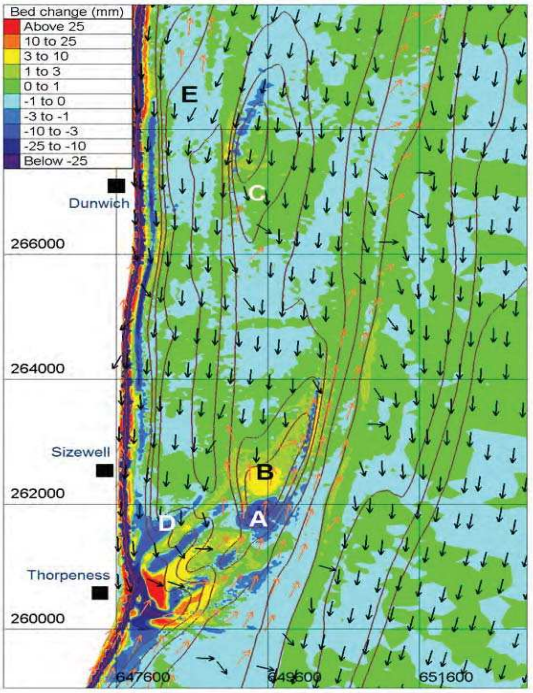


Figure 5: Bedload and suspended load with tidal forcing and annual average waves (Hs = 0.9 m) from north-east sector. Normalised tidal average transport vectors superimposed on erosion deposition patterns (mm) over five M2 tidal cycles. See Figure 3 for explanation of vectors.

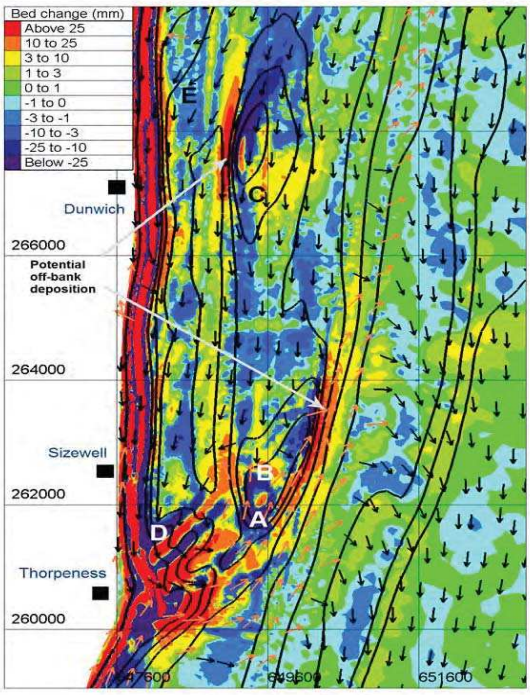


.

Figure 6: Bedload and suspended load with tidal forcing for 1 week return period waves (Hs = 2.2 m) from north-east sector. Normalised tidal average transport vectors superimposed on erosion deposition patterns (mm) over five M2 tidal cycles. See Figure 3 for explanation of vectors.

Calculations with bedload transport only, (Figure 3) showed deposition occurring at the top of the banks (locations B and C) and erosion on the south flank (location A). An interesting feature was the predicted convergence of opposing transport paths from the north and south at the top of the Sizewell Bank. Sediment moving inshore of the bank parallel to the shore was predicted to turn offshore at D, potentially joining material moving up from the south. Also marked is a possible path for material to move offshore from the eastern edge of the bank. Although not evident from the normalised vectors, this pathway is however very weak.

Calculations with bedload and suspended load gave a very similar distribution to the bedload-only case, but with a greater magnitude of erosion and deposition (Figure 4). As with the bedload case, erosion occurred on the southern face of the bank (location A) and the deposition at the top (location B) associated with the transport convergence in this region. As indicated by the normalised vectors, a second (weak) convergence zone is suggested at location C at the northern end of the Sizewell – Dunwich Bank. Thus, under tidal conditions the model yields southward (flood) directed sediment transport in the channel inshore of the Sizewell Bank and northward (ebb) directed transport along the seaward flank of the bank. Over five tidal cycles the magnitude of bed change due to bedload plus suspended load transport is generally in the range from 0-10mm. The similarity in general erosion/deposition pattern is not unexpected as both bedload and suspended load vectors are aligned with the depth mean current, and suspended load magnitude is closely related to the bedload via the reference concentration (3).

### *C. Erosion and deposition with tide and wave forcing*

When a constant annual mean wave forcing was included (Table 1, case 1) the broad scale pattern of erosion and deposition did not change significantly from the tide only case, but magnitudes increased (Figure 5). Note, the inclusion of waves here was as a 'stirring mechanism' i.e. increasing the quantity of sediment being transported but with no modification to currents. Tidal erosion/deposition patterns identified previously were preserved, with erosion occurring on the southern flank (location A) and deposition on the top of the bank at locations B and C. With waves included, net erosion over five tidal cycles near location A for example, increased by a factor of four, from 2.5mm (tide only) to 10.5mm (tide and wave). Similar proportional changes were seen elsewhere. Extrapolation at location A of this magnitude of erosion over a year would give a very significant bed change of around 1.5 m. Bands of erosion and deposition associated with the Coralline Crag (location D) show erosion on the raised 'fingers' and deposition in-between. In this simulation, the start condition had the ridges covered in 10cm of sand, which was completely eroded. This is consistent with observed fluctuations in ridge elevation [16] that suggest that sediment can cover and uncover the ridges. There is also an indication of a bedload parting zone at E, that was present in the tide only calculations, but is more prominent when waves

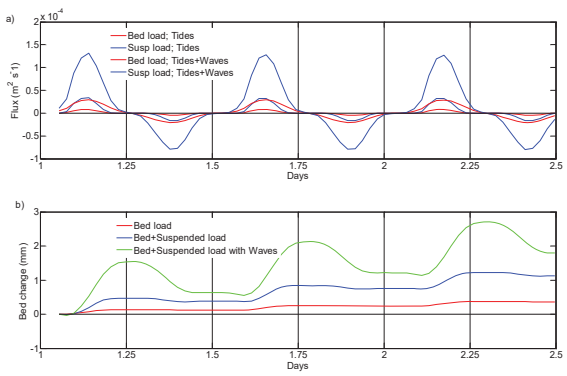


Figure 7: Time series near the top of Sizewell Bank (see Figure 9 for position marked with '+'). a) Sediment flux for bedload, suspended load with and without waves; b) Change in bed elevation. Note the time axis in both graphs is the same so the relationship between the flux and bed response can be discerned.

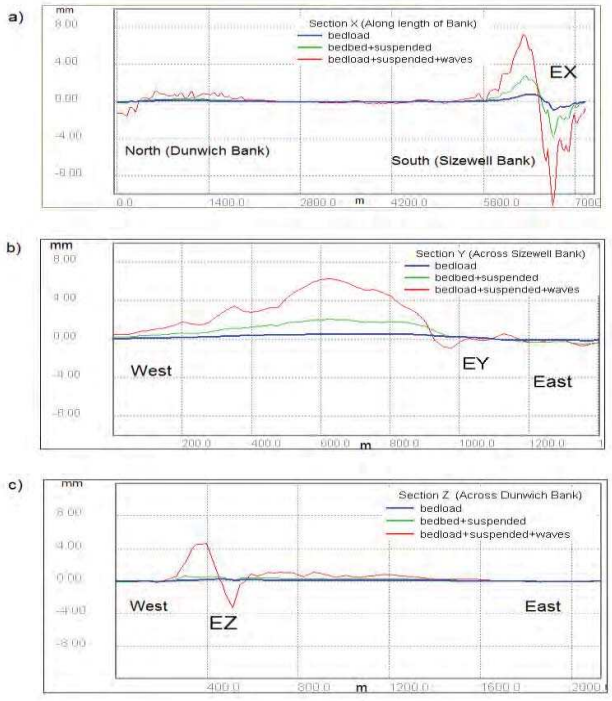


Figure 8: Change in bed elevation for 12 M2 tidal cycles along sections (see Figure 3). a) Section X, N-S along bank, with EX marking the south face of bank; b) section Y, E-W over the Sizewell Bank, with EY marking the east (seaward) face of the bank; c) Section Z, E-W over the Dunwich Bank, with EZ marking the western (shoreward) face of the bank.

are included. It is interesting to note the formation of erosion and deposition bands close to and parallel to the shore, suggestive of the longshore bar that occurs along this stretch of coast. Simulations with waves from the south east sector (Table 1, case 3) shows very similar patterns of erosion and deposition and are not shown here.

With larger waves (Table 1, case2) the overall patterns of erosion/accretion remained broadly similar but with erosion and deposition much intensified (Figure 6). However, the top of the Sizewell bank (location B) that previously showed

accumulation was eroded under stronger waves. Also evident are lateral regions of intense deposition/erosion seaward of the Sizewell Bank and shoreward of the Dunwich Bank. This appears to be a mechanism for removal of bank material in the model simulations. Simulations with waves from the south east sector (Table 1, case 4) showed very similar patterns of erosion and deposition and are not shown here. Note that these simulations neglect the effect of wave driven currents and these will be sensitive to wave direction.

### *D. Further analysis at specific locations along the Bank*

The time series of transport flux magnitude and bed evolution at a location near the top of the Sizewell Bank (cross marked on Figure 2) shows suspended load flux to be about four times the magnitude of bedload flux (Figure 7). Including annual mean wave increased the absolute value of both suspended and bedload flux by approximately a factor of four. Without waves, the tidal transport flux was zero for almost half the tidal cycle, indicating that the average tidal M2 velocities were close to threshold conditions for movement of the sediment class used in the simulation (250 μm diameter). However, when the orbital velocity corresponding to an annual mean wave was included in the Soulsby van Rijn formulae (1), conditions were predicted to be above the transport threshold for most of the tidal cycle. For this location, accumulation of material occurs under both tidal and tide plus (average) wave conditions. Analysis based on the spatial plots (Figure 4 and Figure 5) would suggest the material deposited at the top of the Sizewell Bank is coming from erosion of the southern face.

To look in more detail at the individual effect of bedload, suspended load and wave stirring on bed morphology, the net changes in bed level after 5 tidal cycles were plotted along three transects (marked X, Y, Z Figure 2). Bed level change north-south along the Sizewell-Dunwich Bank system (transect X) in all cases showed erosion of the southern flank and accretion at the top of the Sizewell Bank (Figure 8a). Although hard to discern for the bedload and bedload + suspended load results, there is also some accumulation of material at the northern end on the Dunwich Bank. The effect of wave mobilisation was to enhance this general pattern. The wave-induced mobility also increased the rate of accretion at the Dunwich Bank, pushing it further to the south and removing material on the northern flank. The change in bed level east-west across the Sizewell Bank (transect Y) again shows the accumulation at the top of Sizewell Bank with average wave conditions significantly enhancing this (Figure 8b). However, the wave activity also leads to adjacent bands of erosion and deposition on the eastern (seaward) flank as marked at EY. A similar pattern is also evident in transect Z on the western (shoreward) flank of the Dunwich Bank (Figure 8c). These correspond to the deposition patterns noted in Figure 6 and associated with steep bathymetric gradients with erosion at the top and deposition at the bottom of the slope.

## IV Conclusions

The bedload and suspended load sediment transport regime of the Sizewell Dunwich Bank on the UK east coast was simulated for a range of tidal and wave conditions using the coupled TELEMAC-2D and SISYPHE hydrodynamic and sediment transport model and TOMAWAC spectral wave model. Net sediment flux directions and patterns of erosion and deposition were obtained for the present bank configuration.

The general pattern of tidally averaged total transport flux (bedload plus suspended load) showed a well-defined convergence zone at the location of the present Sizewell Bank. This implies a likely mechanism for bank maintenance, with material moving from the north or the south having the potential to accumulate at the bank location. In particular, the model suggests that sediment transported southward by longshore drift could travel from the nearshore region at Thorpeness to the south end of the bank this providing a mechanism for bank maintenance.

## Acknowledgement

Funding under the British Energy Estuarine and Marine Studies (BEEMS) program and Cefas DP363A funding is gratefully acknowledged. We would also like to thank the many people associated with the BEEMS program who contributed to this work, including Liam Fernand who read the draft manuscript and whose comments helped improve the paper.

## References

[1] M. J. Tucker, A. P. Carr, and E. G. Pitt, “The effect of an offshore bank in attenuating waves,” Coast. Eng., vol. 7, no. 2, pp. 133–144, May 1983.

[2] N. J. MacDonald and B. A. O’Connor, “Influence of Offshore Banks on the Adjacent Coast.,” Proceedings 24th Coast. Eng. Conf., pp. 2311–2324, 1994.

[3] R. J. S. Whitehouse, N. W. Beech, J. A. Roelvink, and S. J. M. H. Hulscher, “Understanding the behaviour and engineering significance of offshore and coastal sand banks.” HR Wallingford Ltd., 1998.

[4] A. Hequette and D. Aernouts, “The influence of nearshore sand bank dynamics on shoreline evolution in a macrotidal coastal environment, Calais, northern France,” Cont. Shelf Res., vol. 30, no. 12, pp. 1349–1361, Jul. 2010.

[5] C. Coughlan, “Hydrodynamic Processes and Sediment Transport around a Headland-Associated Sandbank and Implications for the Neighbouring Shoreline,” 2008.

[6] A. P. Carr, “Evidence for the sediment circulation along the coast of East Anglia,” Mar. Geol., vol. 40, no. 3–4, pp. M9–M22, Apr. 1981.

[7] R. D. Pingree, “The Formation Of The Shambles And Other Banks By Tidal Stirring Of The Seas,” J. Mar. Biol. Assoc. United Kingdom, vol. 58, no. 01, p. 211, Feb. 1978.

[8] L. Maddock and R. D. Pingree, “Numerical simulation of the Portland tidal eddies,” Estuar. Coast. Mar. Sci., vol. 6, no. 4, pp. 353–363, Apr. 1978.

[9] R. D. Pingree and L. Maddock, “The tidal physics of headland flows and offshore tidal bank formation,” Mar. Geol., vol. 32, no. 3–4, pp. 269–289, Jul. 1979.
[10] A. C. Bastos, D. Paphitis, and M. B. Collins, “Short-term dynamics and maintenance processes of headland-associated sandbanks: Shambles Bank, English Channel, UK,” Estuar. Coast. Shelf Sci., vol. 59, no. 1, pp. 33–47, 2004.
[11] V. N. D. Caston, “Linear Sand Banks in the Southern North Sea,” Sedimentology, 1971.
[12] K. R. Dyer and D. A. Huntley, The origin, classification and modelling of sand banks and ridges, vol. 19, no. 10. 1999.
[14] A. Berthot, “Formation and maintenance of headland associated linear sandbanks,” 2005.
[15] A. Berthot and C. Pattiaratchi, “Mechanisms for the formation of headland-associated linear sandbanks,” Cont. Shelf Res., vol. 26, no. 8, pp. 987–1004, 2006.
[16] T. Dolphin, “Sizewell: Morphology of coastal sandbanks and impacts to adjacent shorelines. BEEMS Technical Report TR058, Cefas, Lowestoft.,” 2009.
[17] J. M. Hervouet, “TELEMAC modelling system: an overview,” Hydrol. Process., 2000.
[18] EDF, “TELEMAC Modelling System, 2D hydrodynamics TELEMAC-2D software. User Manual.,” 2014.
[19] K. Vanstaen, “Interpretation of BEEMS Sizewell Swath Bathymetry and Backscatter. BEEMS technical report TR087, Cefas, Lowestoft,” 2010.
[20] D. Garcia, “Robust smoothing of gridded data in one and higher dimensions with missing values,” Comput. Stat. Data Anal., 2010.
[21] R. Soulsby, Dynamics of marine sands : a manual for practical applications. Telford, 1997.
[22] J.-J. Shu, “Prediction and Analysis of Tides and Tidal Currents,” Int. Hydrogr. Rev., vol. 4, no. 2, pp. 57–64, 2003.
[23] R. D. Pingree and D. K. Griffiths, “Sand transport paths around the British Isles resulting from M2 and M4 tidal interactions,” J. Mar. Biol. Assoc. UK, vol. 59, no. 02, pp. 497–513, May 1979.
[24] J. Van Der Molen, “The influence of tides, wind and waves on the net sand transport in the North Sea,” vol. 22, pp. 2739–2762, 2002.
[25] K. Pye and S. J. Blott, “Sea bed sediment characteristics, bedforms and sediment transport pathways in the Sizewell area. BEEMS Technical Report TR107, Cefas, Lowestoft.,” 2011.
[26] EDF, “TELEMAC Modelling System, SYSYPHE, Version 6.3. User Manual.,” 2014.
[27] C. Villaret, J. M. Hervouet, R. Kopmann, U. Merkel, and A. G. Davies, “Morphodynamic modeling using the Telemac finite-element system,” Comput. Geosci., vol. 53, no. September 2014, pp. 105–113, 2013.
[28] E. W. Bijker, “Mechanics of Sediment Transport by the Combination of Waves and Current,” in Proceedings of the Short Course on Design and Reliability of Coastal Structures, 23rd International Conference on Coastal Engineering, 1992.
[29] P. L. Wiberg and C. K. Harris, “Ripple geometry in wave-dominated environments,” J. Geophys. Res., vol. 99, no. C1, p. 775, Jan. 1994.
[30] L. C. van Rijn, D.-J. R. Walstra, and M. van Ormondt, “Unified View of Sediment Transport by Currents and Waves. I: Initiation of Motion, Bed Roughness, and Bed-Load Transport,” J. Hydraul. Eng., vol. 133, no. 7, pp. 776–793, 2007.
[31] G. Galappatti and C. B. Vreugdenhil, “A depth-integrated model for suspended sediment transport,” J. Hydraul. Res., 1985.